J. Fluid Mech. (2013), *vol.* 714, *pp.* 476–488. © Cambridge University Press 2013
doi:10.1017/jfm.2012.493

Available potential energy density for Boussinesq fluid flow

Kraig B. Winters[1,2]† **and Roy Barkan**[1]

[1] Scripps Institution of Oceanography, University of California San Diego, La Jolla, CA 92093, USA

[2] Mechanical and Aerospace Engineering, University of California San Diego, La Jolla CA 92093-0209, USA

(Received 30 March 2012; revised 31 July 2012; accepted 3 October 2012)

An exact expression $\mathscr{E}_a$ for available potential energy density in Boussinesq fluid flows (Roullet & Klein, *J. Fluid Mech.*, vol. 624, 2009, pp. 45–55; Holliday & McIntyre, *J. Fluid Mech.*, vol. 107, 1981, pp. 221–225) is shown explicitly to integrate to the available potential energy E_a of Winters *et al.* (*J. Fluid Mech.*, vol. 289, 1995, pp. 115–128). $\mathscr{E}_a$ is a positive definite function of position and time consisting of two terms. The first, which is simply the indefinitely signed integrand in the Winters *et al.* definition of E_a, quantifies the expenditure or release of potential energy in the relocation of individual fluid parcels to their equilibrium height. When integrated over all parcels, this term yields the total available potential energy E_a. The second term describes the energetic consequences of the compensatory displacements necessary under the Boussinesq approximation to conserve vertical volume flux with each parcel relocation. On a pointwise basis, this term adds to the first in such a way that a positive definite contribution to E_a is guaranteed. Globally, however, the second term vanishes when integrated over all fluid parcels and therefore contributes nothing to E_a. In effect, it filters the components of the first term that cancel upon integration, isolating the positive definite residuals. $\mathscr{E}_a$ can be used to construct spatial maps of local contributions to E_a for direct numerical simulations of density stratified flows. Because $\mathscr{E}_a$ integrates to E_a, these maps are explicitly connected to known, exact, temporal evolution equations for kinetic, available and background potential energies.

Key words: baroclinic flows, computational methods, stratified flows

1. Introduction

Recently, Roullet & Klein (2009) examined a positive definite expression for available potential energy density for Boussinesq fluid flows originally proposed by Holliday & McIntyre (1981), combining it with the specific reference state based on energy minimization (Lorenz 1955) formalized in terms of an adiabatic sorting of fluid parcels discussed in Winters *et al.* (1995).

Roullet & Klein (2009) note that the volume integral of the positive definite expression for energy density yields the same available potential energy E_a of Winters

† Email address for correspondence: kraig@coast.ucsd.edu

https://doi.org/10.1017/jfm.2012.493 Published online by Cambridge University Press

et al. (1995) for which an exact evolution equation is known. This is intriguing, as the formal definition of E_a in Winters *et al.* (1995) is the volume integral of a quantity that is not sign-definite, but rather explicitly accumulates the expenditure or release of energy in moving individual fluid parcels from their actual positions to their equilibrium heights with respect to a globally defined reference density profile. Because the integrand is not sign-definite, it cannot be understood as a local available potential energy density (see e.g. Molemaker & McWilliams 2010).

The objective of this paper is to show the relationship between the exact, positive definite available potential energy density of Roullet & Klein (2009) and the integrand of the available potential energy E_a defined in Winters *et al.* (1995). The positive definite energy density is reinterpreted strictly in terms of the energy released during an adiabatic repositioning of individual fluid parcels, compensated by an opposing, non-local transport of fluid such that the net vertical volume flux vanishes on a parcel-by-parcel basis. Both the volume and the density of the fluid displaced in compensation are uniquely determined by the actual height z and reference height z_* (Winters *et al.* 1995, and § 2 below) of each fluid parcel. This interpretation allows discussion of background potential energy, available potential energy and its local positive definite density strictly in terms of work done in displacing fluid parcels vertically in a gravitational field, a view that seems natural given the usual physical interpretation of potential energy. Although our discussion here is confined to available potential energy under the Boussinesq approximation, similar ideas apply to the mixing of potential vorticity (Wood & McIntyre 2010).

In § 2 we consider a Boussinesq fluid with a linear equation of state, and revisit briefly the definition of available potential energy E_a in a finite volume V and its interpretation in terms of an adiabatic re-sorting of infinitesimal fluid parcels. In § 3 we show that the expression for available potential energy density of Roullet & Klein (2009) can be written as the sum of two terms: the integral definition of E_a of Winters *et al.* (1995), in which the integrand is not sign-definite, and a second integral, also with a sign-indefinite integrand, that integrates identically to zero over V. This second term is described in terms of work against the background pressure force in Holliday & McIntyre (1981) and obtained as a difference of integrands of Casimirs in Roullet & Klein (2009). That it integrates to zero results from the specific property that the reference density profile is an adiabatic redistribution of fluid parcels. Here we reinterpret the work against pressure as additional gravitational work incurred in displacing fluid a small distance to make room for the repositioning of 'flattened' fluid parcels in constructing the one-dimensional reference profile. The integrands describe the two adiabatic resorting operations that, when combined, reveal the positive definite contribution to E_a on a pointwise basis. In § 4 we introduce the fundamental three-dimensional to one-dimensional mapping at the heart of the adiabatic resorting idea, and in §§ 5 and 6 we describe the closed-loop parcel exchanges and compensatory displacement operations underlying the interpretation of the positive definite integrand in terms of resorting. In § 7, we briefly illustrate by example the mechanics of the calculations and their utility using simulations of rotating and non-rotating horizontal convection (see e.g. Hughes & Griffiths 2008). Concluding comments are given in § 8, and a recipe for computing the reference state of minimum potential energy is given in the Appendix.

https://doi.org/10.1017/jfm.2012.493 Published online by Cambridge University Press

2. Available potential energy E_a

The available potential energy E_a is defined in terms of the reference profile $\rho(z_*)$ where z_* is the equilibrium height of a fluid parcel with potential density ρ:

$$E_a \equiv g \int (z - z_*)\rho \, \mathrm{d}V. \tag{2.1}$$

The corresponding definition for total potential energy is

$$E_p(t) \equiv g \int z\rho \, \mathrm{d}V, \tag{2.2}$$

where in both expressions we take z positive upward.

As discussed in Winters *et al.* (1995), the strictly one-dimensional reference profile is defined by

$$z_*(\boldsymbol{x}, t) = \frac{1}{A} \int H[\rho(\boldsymbol{x}', t) - \rho(\boldsymbol{x}, t)] \, \mathrm{d}V', \tag{2.3}$$

where H is the Heaviside step function. For a given point $(\boldsymbol{x}, t)$, the corresponding value z_* is the total volume of fluid in V with density greater than $\rho(\boldsymbol{x}, t)$, normalized by the cross-section A. While it is often convenient to write z_* as an explicit function of space and time, we also note that at fixed t the function z_* has the same unique value at all points on an isopycnal surface. We can therefore regard z_* as a unique function of ρ and consider the corresponding, strictly one-dimensional function $\rho(z_*)$ (at fixed time t). This reference profile is monotonic with $\mathrm{d}\rho/\mathrm{d}z_* \leqslant 0$. The potential energy associated with the reference profile is the global minimum potential energy attainable via adiabatic levelling or sorting of the fluid parcels in V at time t. The definition of background potential energy is therefore

$$E_b \equiv g \int z_*\rho \, \mathrm{d}V, \tag{2.4}$$

which leads immediately to the definition (2.1) since $E_p = E_a + E_b$. Because E_b is the positive definite potential energy after adiabatic levelling, it is intuitively obvious that $E_a > 0$.

That E_a is a positive definite quantity, however, is not at all obvious from the integral expression (2.1) alone. For stratified flows in general, a snapshot of the density field will capture some fluid parcels above their adiabatic equilibrium positions and others below. In particular, $(z - z_*)$ can be of either sign and the total integral represents significant cancellation of positive and negative contributions.

The sign-indefiniteness of the integrand leads to some awkwardness in defining an available potential energy density directly from (2.1). What, for example, is the contribution to E_a from a particle with $(z - z_*) < 0$? The situation here is quite different from that for kinetic energy where the corresponding integrand is positive definite. Each parcel in the domain contributes an identifiable portion of the volume-integrated kinetic energy, and a spatial map of these contributions is intrinsically meaningful.

3. Available potential energy density $\mathscr{E}_a$

It would be useful to define an available potential energy density $\mathscr{E}_a$ with the following properties:

$$g \int \mathscr{E}_a(\boldsymbol{x}, t) \, \mathrm{d}V = E_a(t), \tag{3.1}$$

$$\mathscr{E}_a(\boldsymbol{x}, t) \geqslant 0 \quad \forall \boldsymbol{x}, t. \tag{3.2}$$

https://doi.org/10.1017/jfm.2012.493 Published online by Cambridge University Press

Requirement (3.1) permits a precise physical interpretation of $\mathscr{E}_a$ in the context of the previously known exact evolution equations for E_a and E_b (Winters *et al.* 1995) and their application to diagnosing the energetics of diabatic mixing. Although we will define $\mathscr{E}_a$ formally as a function of $\boldsymbol{x}$ and t, the value for a given parcel can never be a truly local quantity in the sense that the value for each parcel depends on the positions and densities of all other parcels via a dependence on $z_*(\rho)$. Nevertheless, with requirement (3.2), the spatial distribution of the local contributions can be examined. Such an expression would also allow, for example, a spectral decomposition and an assessment of the scale dependence of available potential energy as in Molemaker & McWilliams (2010).

We define the available potential energy density as follows:

$$\mathscr{E}_a(\boldsymbol{x}, t) \equiv (z - z_*)(\rho(\boldsymbol{x}, t) - \overline{\rho}(z, z_*)), \tag{3.3}$$

where

$$\overline{\rho}(z, z_*) = \frac{1}{(z - z_*)} \int_{z_*}^{z} \rho(z'_*)\, \mathrm{d}z'_*. \tag{3.4}$$

Equation (3.3) is equivalent to (2.1) of Roullet & Klein (2009) when z_r in that paper is taken as z_* and ρ_r as the reference profile $\rho(z_*)$. Roullet & Klein (2009) also show by way of a Taylor series that, in the limit of small displacements from the reference state, (3.3) reduces to their quadratic quasi-geostrophic expression (2.3).

The first thing to note is that $\mathscr{E}_a \geqslant 0$, vanishing only for fluid parcels located at their equilibrium heights. Figure 1 shows schematically a monotonic reference profile $\rho(z_*)$ for a given flow at time t. We now consider two possibilities for the fluid parcel located at height $z = z_i$ with a density value ρ_i. In constructing the reference profile from discrete volume elements, each parcel with volume $\mathrm{d}V = \mathrm{d}x\,\mathrm{d}y\,\mathrm{d}z$ is first 'flattened' to size $A\,\mathrm{d}z_*$. The flattened parcels, each with thickness $\mathrm{d}z_* = \mathrm{d}V/A \ll \mathrm{d}z$, are then stacked in order of descending density. Figure 1(*a*) illustrates the case where the position of the parcel at time t is higher than its equilibrium location $z_*(\rho_i)$. The horizontal position of the parcel is not relevant to the argument. In this case, $(z_i - z_*) > 0$ and the density $\overline{\rho}(z_i, z_*)$ is the average of the reference profile over a range of heights greater than $z_*(\rho_i)$ and so must be less than ρ_i. Thus, the product in (3.3) is positive for all such parcels. Similarly, figure 1(*b*) illustrates the case for a parcel located below its equilibrium position. The average density $\overline{\rho}$ is greater than $\rho(z_i)$ but now represents an average over a portion of the reference profile below $z_*(\rho_i)$. Thus, the two terms in (3.3) are both negative and the product is once again positive. The definition (3.3) therefore satisfies requirement (3.2).

To show that (3.3) also satisfies (3.1), we first rewrite the integral for E_a as

$$E_a = g \int \mathscr{E}_a(\boldsymbol{x}, t)\, \mathrm{d}V = g \int (z - z_*)\rho(\boldsymbol{x}, t)\, \mathrm{d}V - g \int \int_{z_*}^{z} \rho(z'_*)\, \mathrm{d}z'_*\, \mathrm{d}V. \tag{3.5}$$

Denoting the last two integrals in (3.5) as $\mathscr{I}_1$ and $\mathscr{I}_2$ respectively, establishing (3.1) is equivalent to showing that $\mathscr{I}_2 = 0$.

Consider the contribution to $\mathscr{I}_1$ and $\mathscr{I}_2$ associated with the ith parcel with volume element $\mathrm{d}V$ located at height z_i with density ρ_i. The contribution to $\mathscr{I}_1$ from this parcel is the energy expended or released in moving the ith parcel from its actual height z_i to its equilibrium position $z_*(\rho_i) \equiv z_*^i$:

$$\mathscr{I}_1^i = g\,\mathrm{d}V\,\rho_i(z_i - z_*^i). \tag{3.6}$$

https://doi.org/10.1017/jfm.2012.493 Published online by Cambridge University Press

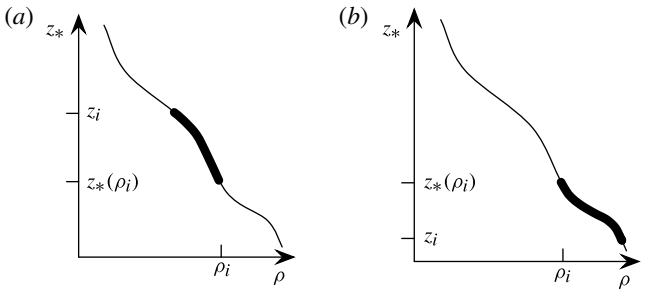


FIGURE 1. $\mathscr{E}_a$ (equation (3.3)) is positive definite: (*a*) $(z_i - z_*) > 0$, $\rho(z_i) - \overline{\rho}(z_i, z_*) > 0$; (*b*) $(z_i - z_*) < 0$, $\rho(z_i) - \overline{\rho}(z_i, z_*) < 0$.

Relocation of this parcel represents a 'volume displacement' of $(z_i - z_*^i) \times \mathrm{d}V\,\mathrm{m}^4$, either upward or downward depending on the sign of $(z_i - z_*^i)$.

Similarly,

$$\mathscr{I}_2^i = -g\,\mathrm{d}V \int_{z_*^i}^{z_i} \rho(z'_*)\,\mathrm{d}z'_* \approx -g\,\mathrm{d}V \sum_{j=1}^{n} \rho_j\,\Delta z_* = -g\Delta z_* \sum_{j=1}^{n} \rho_j\,\mathrm{d}V \tag{3.7}$$

where n is the number of $\mathrm{d}V$ parcels with height in the reference density profile between z_*^i and z_i. The increment Δz_* is a signed quantity with magnitude $\mathrm{d}z_* = \mathrm{d}V/A$. $\mathscr{I}_2^i$ is thus the energy expended or released in moving the particular volume of fluid, with density either somewhat greater than or somewhat less than ρ_i, a small distance Δz_* to make room for parcel i. Schematically, this corresponds to the energy associated with shifting the parcels comprising the thick portions of the reference profiles in figure 1 a small distance Δz_*. The sign of the shift again depends on the sign of $(z - z_*)$, but it is always opposite to the direction implied by the relocation of parcel i from z to z_*. As the volume displacement of these parcels is equal to $-(z - z_*) \times \mathrm{d}V$, $\mathscr{I}_2^i$ gives the energetic consequences of the particular compensatory displacement required in moving parcel i to its equilibrium position. We have already seen that, taken together, $\mathscr{I}_1^i + \mathscr{I}_2^i \geqslant 0$ for any parcel i.

4. Equivalent energy three-dimensional to one-dimensional map

It remains to be shown that $\mathscr{I}_2$ is equal to zero. Extending the interpretation of the previous section, we continue with a discrete approach and consider the integrations over the volume V as a sequence of reordering operations involving the discrete parcels with volume elements $\mathrm{d}V$ and passing to the limit $\mathrm{d}V \to 0$. To simplify the presentation, however, it is first necessary to introduce a nearly energy-conserving mapping of the mass distribution $\rho(\boldsymbol{x})$ at time t to a strictly one-dimensional distribution $\rho_{1D}(z)$.

The potential energy associated with the parcel located at (x, y, z) depends on the height z but is independent of the horizontal position. Furthermore, for small $\mathrm{d}V$ elements, we have seen that $\mathrm{d}z_* \ll \mathrm{d}z$. The profile $\rho_{1D}(z)$ is constructed by taking all the $\mathrm{d}V$ elements located at a given height z, 'flattening' them to occupy a volume $A \times \mathrm{d}z_*$ and placing them arbitrarily within the height range $[z, z+\mathrm{d}z]$. For each parcel i, the magnitude of the difference in potential energy between the three-dimensional and one-dimensional configurations is bounded by $g\,\mathrm{d}V\rho_i\,\mathrm{d}z$, which vanishes like $\mathrm{d}z^2$ as $\mathrm{d}V \to 0$. The potential energy associated with $\rho_{1D}(z)$ is therefore arbitrarily close to E_p

https://doi.org/10.1017/jfm.2012.493 Published online by Cambridge University Press

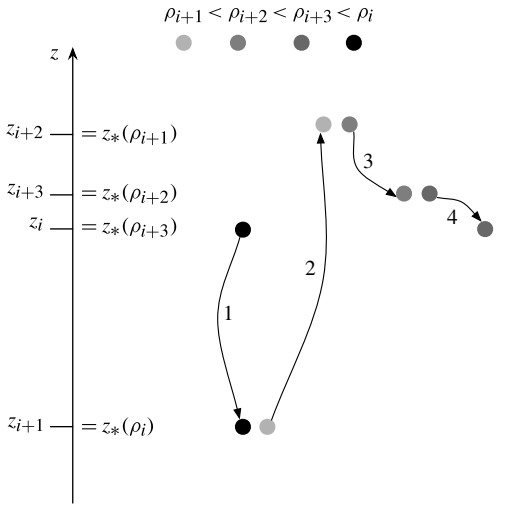


FIGURE 2. Schematic representation of the four-step closed-loop exchange described in the text. Starting with the parcel located at z_i, parcels are moved to their equilibrium heights z_*, replacing the parcels previously located at those locations. The replaced particles are then moved to their equilibrium positions. The parcel exchanges continue until the parcel with equilibrium position z_i replaces the original parcel and the loop is closed.

in (2.2) for small but finite $\mathrm{d}V$ and equal to E_p in the limit. The important point here is that the flattened elements are geometrically conformable with those in the reference state $\rho(z_*)$, which can now be formally constructed from $\rho_{1D}(z)$ via a sequence of discrete parcel interchanges. In principle, we can track the energetic consequences of both the direct equilibration of individual parcels ($\mathscr{I}_1^i$) as well as that of the 'compensatory displacement' operations ($\mathscr{I}_2^i$) associated with each such repositioning. We show, however, that the accumulated distance in compensatory displacement of each parcel, i.e. displacements 'induced' by the direct relocation to equilibrium of all other parcels, sums to zero. This implies that the net energy released in compensatory displacements vanishes for each parcel individually and therefore, in the limit $\mathrm{d}V \to 0$, that $\mathscr{I}_2 = 0$.

5. Closed-loop exchanges

The monotonic reference profile $\rho(z_*)$ can be obtained from $\rho_{1D}(z)$ via a finite sequence of *closed-loop parcel exchanges* that produces a reordering of the given sequence of density values such that the heaviest parcel is placed at the bottom of the volume, the next heaviest just above, and so on. The general algorithm for computing $\rho(z_*)$ is given in the Appendix. The idea of closed-loop exchanges is illustrated by means of a sequence of parcel exchanges that closes after four steps, as shown in figure 2. Absent additional restrictions on the underlying flow, we regard the profile $\rho_{1D}(z)$ as a random sequence of the density values ρ observed in V at time t. Suppose we select a random parcel located at position z_i with density ρ_i and calculate the equilibrium position $z_*(\rho_i)$ for this parcel.

Following the schematic in figure 2, we introduce the following interchange operations.

https://doi.org/10.1017/jfm.2012.493 Published online by Cambridge University Press

(i) Move parcel ρ_i from z_i to $z = z_*(\rho_i)$. Label the parcel previously located at $z = z_*(\rho_i)$ with index $i + 1$.

(ii) Move parcel ρ_{i+1} from z_{i+1} to $z = z_*(\rho_{i+1})$. Label the parcel previously located at $z = z_*(\rho_{i+1})$ with index $i + 2$.

(iii) Move parcel ρ_{i+2} from z_{i+2} to $z = z_*(\rho_{i+2})$. Label the parcel previously located at $z = z_*(\rho_{i+2})$ with index $i + 3$.

(iv) Move parcel ρ_{i+3} from z_{i+3} to $z = z_*(\rho_{i+3})$.

This particular sequence of exchanges closes after four steps because the unique parcel with equilibrium position matching the randomly chosen initial parcel was encountered, i.e. $z_*(\rho_{i+3}) = z_i$. We call such a sequence a closed-loop exchange. The number of steps in a closed-loop exchange is greater than or equal to one. A complete reordering, i.e. the construction of $\rho(z_*)$ from $\rho_{1D}(z)$, can always be accomplished through a finite sequence of closed-loop exchanges of varying lengths, initiated with a randomly chosen parcel.

6. Compensatory displacements

Recall that for each parcel relocation from z_i to z_*^i implied by (2.1) and explicitly represented by $\mathscr{I}_1^i$, a compensating displacement over a small distance $\mathrm{d}z_*$ has been introduced via $\mathscr{I}_2^i$ involving all fluid parcels with equilibrium heights between z_i and z_*^i. For a given parcel i, the two relocation operations together always result in a release of energy, i.e. $\mathscr{E}_a > 0$, unless parcel i happens to be located at its equilibrium height, in which case $\mathscr{E}_a = 0$.

While an individual parcel has only one primary relocation, from its initial height z_i to its height in the reference profile z_*^i, it is generally subject to multiple additional translations as a member of different density classes undergoing compensatory displacement, as discussed above. Figure 3 illustrates these motions for the four-step closed-loop exchange sequence introduced in § 5. The arrows indicate translation of specific sets of parcels, either upward or downward, by a distance $\mathrm{d}z_*$ in association with the primary parcel relocation at each step shown in figure 2. In this example, each parcel is involved in exactly two compensatory translations, one up and one down, so that the total distance travelled by each parcel as a result of these translations is zero.

The cancellation of translations is a direct consequence of the fact that the four primary translations i to $i + 3$ form a closed-loop exchange sequence. The net translation during compensatory displacement for all parcels is always zero for closed-loop exchange sequences regardless of their length. Because a complete reordering can always be obtained via a finite sequence of closed-loop exchanges, it follows that the net compensatory translation of all parcels during the reordering is identically zero and therefore $\mathscr{I}_2$ is identically zero.

By introducing $\mathscr{I}_2$ into the definition of $\mathscr{E}_a$ we have added the particular function of $\boldsymbol{x}$ that, when added to $\mathscr{I}_1^i$, yields a positive definite contribution to the available potential energy for each parcel i, while, once integrated over all parcels, it does not contribute to the total integral E_a. In essence, $\mathscr{I}_2$ filters out the cancellation inherent in the integrand (2.1) and isolates the unique positive definite contribution from each spatial location.

https://doi.org/10.1017/jfm.2012.493 Published online by Cambridge University Press

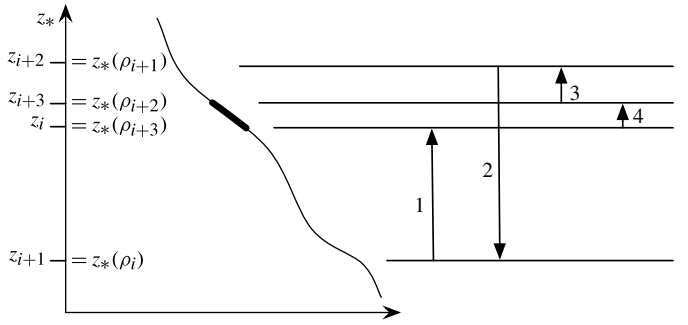


FIGURE 3. Compensatory displacements for the four-step closed-loop exchange sequence shown in figure 2 and described in the text. The upward arrow labelled 1 indicates the upward transport of all fluid with density between ρ_{i+3} and ρ_i over a distance $\mathrm{d}z_*$ which comprises the compensatory displacements in $\mathscr{I}_2^i$ for parcel i. The same parcels are moved an equivalent distance downward as part of the compensatory displacements for parcel $i+1$. Similarly, the parcels within the density range indicated by the heavy line portion of the curve are moved down and up a distance $\mathrm{d}z_*$ during the compensatory displacements for steps 2 and 4 respectively. All fluid parcels experience a zero net compensatory displacement for a closed-loop exchange sequence.

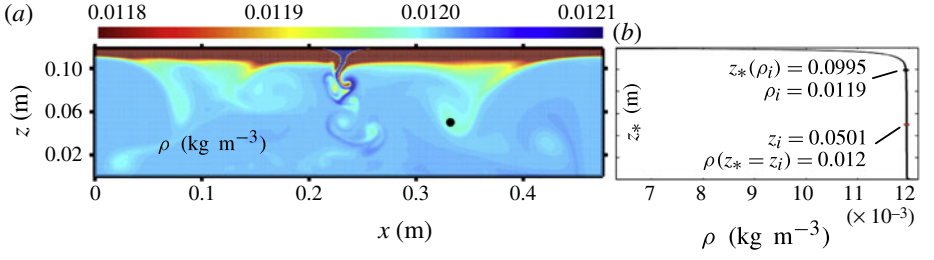


FIGURE 4. (*a*) Snapshot of density field from a numerical simulation of horizontal convection illustrating the calculations associated with a single fluid parcel (black circle) with density $\rho = \rho_i$ located at $z = z_i$, at time t. (*b*) The corresponding reference profile $\rho(z_*)$ associated with the minimum potential energy state attainable via adiabatic sorting. The red circle shows the density of the fluid parcel located at z_i in the sorted profile, $\rho(z_* = z_i)$.

7. Application to rotating horizontal convection

Horizontal convection is the term used to describe the buoyancy-driven flow that results when a fluid is subjected to horizontally variable buoyancy forcing at either its top or bottom surface (see Hughes & Griffiths 2008). The flows that result are generated entirely by the conversion of available potential energy to kinetic energy through the buoyancy flux (e.g. Winters & Young 2009) and so knowledge of the spatial distribution of $\mathscr{E}_a$ in these flows is of fundamental interest. Figure 4(*a*) shows the density field from a two-dimensional simulation of horizontal convection with temperature prescribed at the upper boundary such that the fluid is heated at the left and right portions of the upper surface and cooled in the middle. This snapshot will be used to illustrate the analytical formulae introduced in the previous discussion.

The black circle in figure 4(*a*) indicates the vertical position $z_i = 0.0501$ m of fluid parcel i with density $\rho_i = 0.0119$ kg m^{-3}. The black circle in figure 4(*b*) shows

https://doi.org/10.1017/jfm.2012.493 Published online by Cambridge University Press

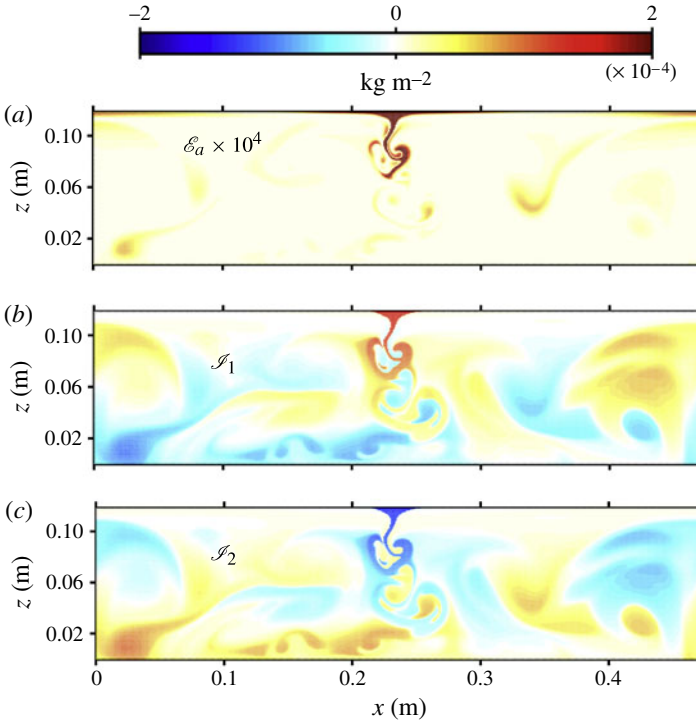


FIGURE 5. Integrands for (*a*) $\mathscr{E}_a$, (*b*) $\mathscr{I}_1$ and (*c*) $\mathscr{I}_2$ as a function of x and z. $\mathscr{E}_a$ is multiplied by 10^4.

that the corresponding equilibrium height for this parcel in the reference profile is $z_*(\rho_i) = 0.0995$ m, which is above z_i (the red circle). Parcel i must therefore be moved a distance $(z_*(\rho_i) - z_i)$ upward during an adiabatic sorting to the minimum energy state. This corresponds to a 'volume displacement' of $\mathrm{d}V \times (z_*(\rho_i) - z_i) = 2.228 \times 10^{-8}$ m^4 for the particular discrete interior parcel size for this simulation. The average $\bar{\rho}$, defined in (3.4), is the average density of the fluid between the red and black circles in figure 4(*b*). The total volume of fluid within the density range is equal to $(z_*(\rho_i) - z_i) \times A$, and the corresponding volume flux when lowering this fluid the small distance $\mathrm{d}z_* = \mathrm{d}z/A$ exactly cancels that associated with equilibrating parcel i.

These two relocation operations, equilibration of a single parcel and the corresponding compensatory displacement, are the two operations implied by the integrands of $\mathscr{I}_1$ and $\mathscr{I}_2$ respectively. Carrying out these operations pointwise throughout the domain yields the spatial maps shown in figure 5. Figure 5(*a*) shows $10^3 \times \mathscr{E}_a$ as defined in (3.3), which characterizes the essential contribution from each parcel to the volume-integrated available potential energy E_a. The available potential energy density is concentrated in the middle of the domain in the cool fluid that is ejected from the upper surface as a negatively buoyant plume. Figure 5(*b*) shows $(z - z_*)\rho$, the integrand of $\mathscr{I}_1$ in (3.5), which integrates to the same value as the function shown in figure 5(*a*) but exhibits both positive and negative values with much larger magnitudes. Integrating this function over the domain produces significant cancellation, which prevents identification of the essential contribution on a pointwise basis. Figure 5(*c*) shows $-(z - z_*)\bar{\rho}$, the integrand for $\mathscr{I}_2$. This function accounts

https://doi.org/10.1017/jfm.2012.493 Published online by Cambridge University Press

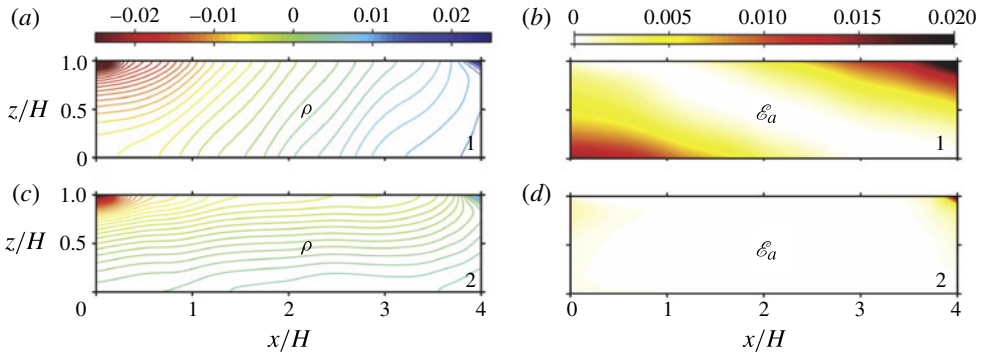


FIGURE 6. (*a,c*) The *y*-averaged snapshots of density ρ, normalized by $\rho_0 B_{max} H/g\kappa$. (*b,d*) The corresponding *y*-averaged available potential energy density normalized by $\rho_0 B_{max} H^2/g\kappa$. (*a,b*) State 1, (*c,d*) state 2.

for the compensatory displacements associated with each direct parcel relocation. Pointwise it is always opposite in sign to the function in figure 5(*b*). In the absence of discretization errors, the volume integral of this function would be identically zero. In this example, the integral $\mathscr{I}_2$ is a small fraction of E_a:

$$\frac{\left|\int -(z-z_*)\,\bar{\rho}\,\mathrm{d}V\right|}{\int (z-z_*)\,\rho\,\mathrm{d}V} \approx 1\times 10^{-3}. \tag{7.1}$$

Figure 6 shows results from a three-dimensional simulation of rotating horizontal convection. In this example, positive heat flux is applied at the upper left, negative heat flux at the upper right and the entire domain rotates about the vertical axis. The non-dimensional parameters defining this simulation (see Hughes & Griffiths 2008) are the flux Rayleigh number $Ra_f \equiv B_{max} L_x^4/\nu\kappa^2 = 3.8\times 10^9$, the Prandtl number $Pr \equiv \nu/\kappa = 7$, the aspect ratio $H/L_x = 0.25$ and the rotation rate $Q \equiv f\,L_x^2/\nu Ra_f^{1/3} = 9.5$ (see Barkan, Winters & Llewellyn-Smith 2012). Here B_{max} is the maximal buoyancy flux applied at the top surface, f is the Coriolis frequency, L_x is the domain length in the $\boldsymbol{x}$ direction, and ν and κ are molecular diffusivities for momentum and temperature respectively. The initial conditions for this three-dimensional simulation were the steady-state solutions from a two-dimensional simulation with identical parameters. In two dimensions, the addition of sufficiently rapid rotation inhibits lateral spreading of dense fluid at depth, producing a geostrophically balanced flow characterized by relatively high available potential energy density beneath the cooled portion of the upper surface. Once perturbations are introduced and three-dimensional flow is allowed to develop, baroclinic instability ensues, releasing the stored available potential energy. Because of the high available potential energy content of these initial conditions, the ensuing flow undergoes a quasi-periodic oscillation between two distinct states. Figure 6(*a,c*) shows the *y*-averaged density and figure 6(*b,d*) the corresponding *y*-averaged $\mathscr{E}_a$ for each of these states. State 1 has high values of available potential energy owing to the sloping isopycnals while in state 2 the available potential energy has been almost completely released via baroclinic instability. Figure 7 shows the volume-integrated available potential energy E_a as the flow oscillates between the two states. Initially E_a is 5–6 times larger than in the rest of the simulation due

https://doi.org/10.1017/jfm.2012.493 Published online by Cambridge University Press

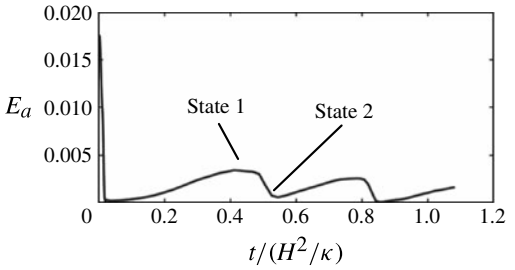


FIGURE 7. E_a, normalized by $\rho_0 V B_{max} H^2/\kappa$, as a function of time. E_a decreases rapidly owing to baroclinic instability. This rapid transient is followed by a slowly decaying oscillation between states 1 and 2.

to the excess available potential energy stored in the two-dimensional flow when baroclinic instability cannot occur. Once the initial excess available potential energy is released, the flow develops quasi-steady oscillations which decay slowly in time. This slow decay shows that most of the energy is being exchanged between kinetic and available potential energies, and only a small fraction is being dissipated or expended in irreversible mixing.

8. Discussion

An exact, positive definite available potential energy density $\mathscr{E}_a$ (Holliday & McIntyre 1981; Roullet & Klein 2009; Molemaker & McWilliams 2010) for stratified flows under the Boussinesq approximation has been shown to integrate to the expression for E_a in Winters *et al.* (1995) and to have a physical interpretation in terms of adiabatic redistribution of fluid parcels and the corresponding positive definite release of potential energy. The expression is exact in the sense that it does not rely on a small perturbation approximation for the displacements, nor a near-linearity approximation for the reference profile. Independence from a small perturbation approximation has advantages both for small-scale turbulent flows, where parcel excursions can be large compared to eddy scales, and for larger-scale ocean flows, where the curvature of the reference profile is often significant (Roullet & Klein 2009). The explicit connection to E_a allows a rigorous interpretation of $\mathscr{E}_a$ in terms of the volume-integrated energy transfers between kinetic energy and available and background components of potential energy described in the evolution equations of Winters *et al.* (1995).

The concepts of available potential energy are quite useful for understanding the dynamics of horizontal convection. In horizontal convection, the fluid is energized by a diffusive flux of available potential energy through the upper surface (Hughes, Hogg & Griffiths 2009; Winters & Young 2009). The interpretation of E_a in terms of the energy released under the action of two resorting operations, i.e. the repositioning of a given parcel and the corresponding compensatory displacements required, and the spatial distribution of $\mathscr{E}_a$ allows one to see at a glance that state 2 in figure 6 represents a nearly complete release of available potential energy while also illustrating where in the flow the baroclinic instability is ineffective at releasing available potential energy. The energy transfers are similar to those discussed by Molemaker & McWilliams (2010) for an Eady-like (Eady 1949) shear flow.

Finally, we note that while the development presented here is formally valid for simple container shapes with uniform cross-section A, it is straightforward to compute

https://doi.org/10.1017/jfm.2012.493 Published online by Cambridge University Press

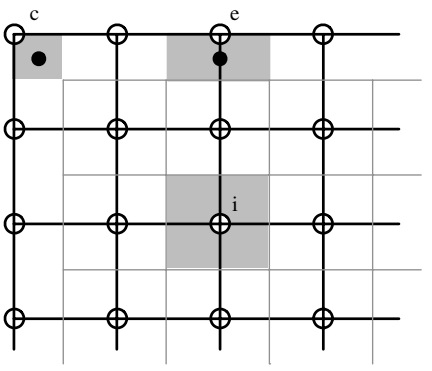


FIGURE 8. Schematic of a discrete grid (collapsed to two dimensions) with density values given at the grid points shown as open circles. Interior grid points (labelled i) give the density values at the centre of discrete volume elements of size dV (shaded). Density values near edges (e), seams and corners (c) are interpolated to their respective volume centres (solid circles). These volume elements have sizes equal to one-half, one-quarter and one-eighth dV respectively. (Here corner volume elements are bounded by three edge faces, seams by two and edges by one.)

the corresponding quantities for irregular numerical discretizations and/or in more complicated single-basin geometries by taking dV to be a function of position and A to be a function of height z. For irregularly shaped containers, i.e. those with tall sills or obstructions, Stewart (2012) suggests defining the reference state in terms of a local minimum of potential energy rather than the global minimum discussed here. Local minima reflect re-sortings in which dense fluid parcels are sorted and stacked within their local basin, even if additional potential energy would be released by allowing the parcel to be positioned in a different, perhaps deeper basin. Such local minima may be useful, for example, when the energy required to move deep dense parcels from one basin to another is large compared to the typical kinetic energy of the flow.

Acknowledgements

Discussions with Myrl Hendershott were much appreciated and gratefully acknowledged. We also appreciate the helpful suggestions of J. Nycander. This work was supported by the National Science Foundation (grants OCE-0726320 and OCE-0926481).

Appendix. Calculation of the reference profile

We describe here our implementation of the construction of the one-dimensional reference state $\rho(z_*)$ from a snapshot of the three-dimensional Boussinesq density field obtained from a numerical model. For specificity, we assume that the numerical model generates density values at regularly spaced discrete grid points in a simple domain of size $L_x \times L_y \times L_z$. Let $A = L_x L_y$ be the cross-sectional area of the domain and let $\mathrm{d}V = \mathrm{d}x\,\mathrm{d}y\,\mathrm{d}z$ be the nominal discrete differential unit of volume. The reference state is simply the mapping between height z_* and density ρ corresponding to a global minimum in potential energy defined by (2.3). We construct this state using a simple sorting and stacking procedure.

https://doi.org/10.1017/jfm.2012.493 Published online by Cambridge University Press

Let the density value at each interior grid point i represent the differential volume element centred at the grid point as shown in figure 8. All such elements have a volume $\mathrm{d}V$. Edge elements adjacent to the boundaries are similar, except that they occupy only half the volume $\mathrm{d}V$, and the density values at the volume centres are not directly available from the model output but rather are found by interpolation. Similarly, the seam and corner elements occupy one-quarter and one-eighth the volume of the interior elements.

Mapping to a discrete one-dimensional profile can be thought of as 'squashing' each volume element $\mathrm{d}V_i$ into a thin sheet of thickness $\mathrm{d}z_{*i} = \mathrm{d}V_i/A$ and assigning its central density value ρ_i to a particular height z_{*i}. The first step is to determine the central density values ρ_i for all the edge, seam and corner elements, keeping track of the corresponding value $\mathrm{d}z_{*i}$. The set of discrete density values is then sorted in order of decreasing density. The densest parcel is placed at the bottom of the domain and assigned a height value of $\mathrm{d}z_{*i}/2$. The rest of the parcels are then stacked in order with each parcel j assigned a z_* value of $z_{*j-1} + \mathrm{d}z_{*j-1}/2 + \mathrm{d}z_{*j}/2$. The result is a monotonic mapping of ρ to z_* expressed on a discrete z_* 'grid' that is unequally spaced owing to the different-sized volume elements at the edges, seams and corners of the domain. This approach is easily adapted to different gridding schemes and irregular domains. It obviates the unnecessary step of first distributing the sorted parcels onto horizontal planes and then approximately removing the remaining available potential energy by averaging.

REFERENCES

Barkan, R., Winters, K. B. & Llewellyn-Smith, S. G. 2012 Rotating horizontal convection. *J. Fluid Mech.* (submitted).

Eady, E. 1949 Long waves and cyclone waves. *Tellus* **1**, 33–52.

Holliday, D. & McIntyre, M. E. 1981 On potential energy density in an incompressible, stratified fluid. *J. Fluid Mech.* **107**, 221–225.

Hughes, G. O. & Griffiths, R. W. 2008 Horizontal convection. *Annu. Rev. Fluid Mech.* **40**, 185–208.

Hughes, G. O., Hogg, A. M. & Griffiths, R. W. 2009 Available potential energy and irreversible mixing in the meridional overturning circulation. *J. Phys. Oceanogr.* **39**, 3130–3146.

Lorenz, E. N. 1955 Available potential energy and the maintenance of the general circulation. *Tellus* **7**, 157–167.

Molemaker, M. J. & McWilliams, J. C. 2010 Local balance and cross-scale flux of available potential energy. *J. Fluid Mech.* **645**, 295–314.

Roullet, G. & Klein, P. 2009 Available potential energy diagnosis in a direct numerical simulation of rotating stratified turbulence. *J. Fluid Mech.* **624**, 45–55.

Stewart, K. D. 2012 The effect of sills and mixing on the meridional overturning circulation. PhD thesis, Australian National University (in press).

Winters, K. B., Lombard, P. N., Riley, J. J. & D'Asaro, E. A. 1995 Available potential energy and mixing in density stratified fluids. *J. Fluid Mech.* **289**, 115–128.

Winters, K. B. & Young, W. R. 2009 Available potential energy and buoyancy variance in horizontal convection. *J. Fluid Mech.* **629**, 221–230.

Wood, R. B. & McIntyre, M. E. 2010 A general theorem on angular-momentum changes due to potential vorticity mixing and on potential-energy changes due to buoyancy mixing. *J. Atmos. Sci.* **67**, 1261–1273.

https://doi.org/10.1017/jfm.2012.493 Published online by Cambridge University Press